

## SUPPORTING INFORMATION

### **Uncatalyzed N-Alkylation of Amines in Ionic Wind from Ambient Corona Discharge**

*Suji Lee, Dmytro S. Kulyk, Nicholas Marano, and Abraham K. Badu-Tawiah\**

Department of Chemistry and Biochemistry  
The Ohio State University  
Columbus, Ohio 43210

\*Corresponding Author:  
Prof. Abraham Badu-Tawiah:  
Tel.: (614) 929-4276  
Email: [badu-tawiah.1@osu.edu](mailto:badu-tawiah.1@osu.edu)

Supporting information is summarized in the table below

<b>Topic</b>	<b>Title of Topic</b>	<b>Pages</b>
Title and TOC		S-1 – S-2
<b>Topic 1</b> (Fig. S1)	Materials and explanation of detailed experimental conditions	S-3
<b>Topic 2</b> (Fig. S2)	Comparison of survival yield (%) for two different configurations of plasma sources	S-4
<b>Topic 3</b> (Fig. S3)	Tandem MS analysis of degradation product from n-butylamine N-alkylation reactions	S-4
<b>Topic 4</b> (Fig. S4)	Surface effect studies utilizing Ag, Ir, and Pt/Ru electrodes	S-5
<b>Topic 5</b> (Fig. S5)	Online screening for other linear and cyclic aliphatic amines	S-6
<b>Topic 6</b> (Sch. S1, Fig.S6-S8)	Cross-coupled N-alkylation between benzylamine and hexylamine	S-7 – S-8
<b>Topic 7</b> (Sch. S2)	Possible mechanism of solution-phase reactions involving collected ionic species from the ionic wind	S-9
<b>Topic 8</b> (Fig. S9)	Estimation of the amounts of N-benzylidenebenzylamine collected from the gas-phase reaction using benzylamine vapor	S-9
<b>Topic 9</b> (Fig. S10-S13)	Orbitrap MS spectra of online screening N-alkylation of amines	S-10 – S-11
<b>Topic 10</b> (Table S1)	Chemical structures and relative abundances of products from online N-alkylation of all amines examined	S-12
<b>Topic 11</b> (Table S2)	Chemical structures and relative abundances of products from online cross-coupled N-alkylation between benzylamine and hexylamine	S-13
<b>Topic 12</b>	References	S-13

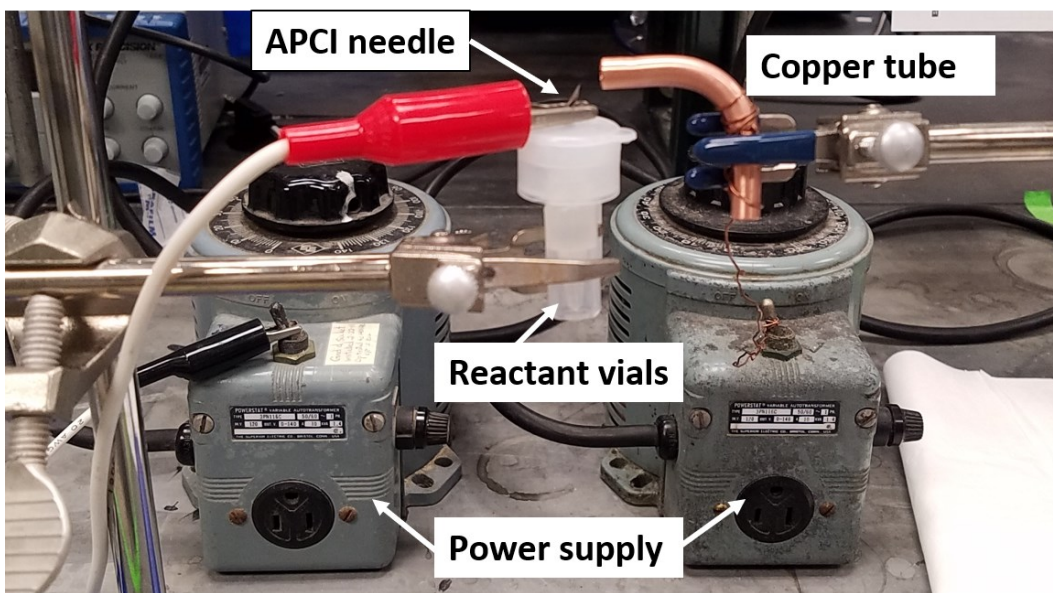
## 1. Materials and explanation of detailed experimental conditions

### Online atmospheric pressure ion-molecule reaction screening

Polyethylene main container (internal volume, 7 mL) and polypropylene sample vial (600  $\mu$ L) were purchased from Fisher Scientific Co. (Hampton, NH). Borosilicate glass capillaries (0.86 mm I.D., 10 cm L) were purchased from Sutter Industries (Novato, CA). Metal wire electrodes (Ag and Ir) were used for online APCI reaction screening, especially for studying if surface effect takes a role on reaction. Silver wire electrode holder (1.5 mm O.D.) was purchased from Warner Instruments (Hamden, CT), iridium wire (0.15 mm diameter, 0.29990 ohms/cm) was purchased from Scientific Instrument Services, Inc (Ringoes, NJ). Pt/Ru LW6 (.006 Inch/ 34 Ga/ 0.15 mm diameter) was purchased from Hoover & Strong.

### Offline product collection

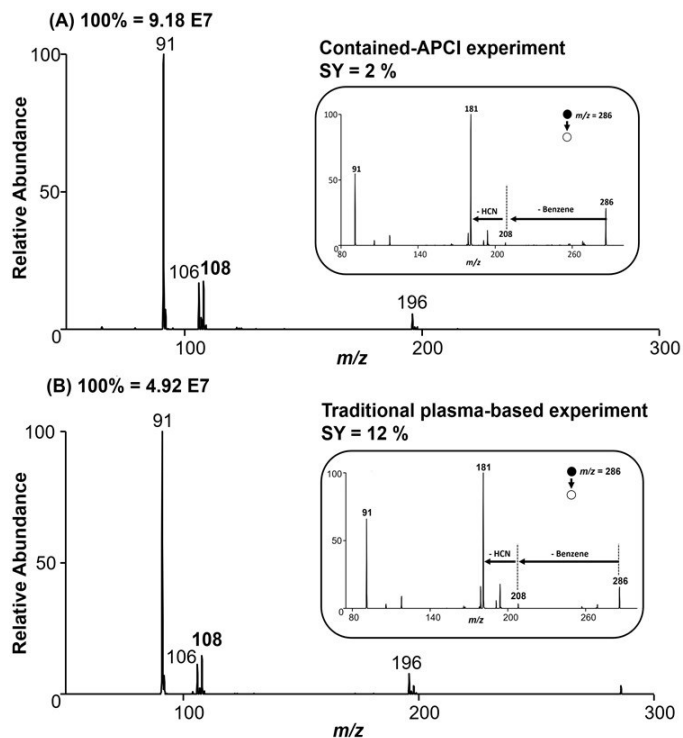
Instead of using metal electrodes that used on online atmospheric pressure ion-molecule reaction screening apparatus, sharp needle was used for offline collection atmospheric pressure ion-molecule reaction products (Figure 1B and Figure S1). Apparatus for collector was made of copper tubing (6.35 mm O.D., 67 mm L), which was purchased from Alfa Alsar (Ward Hill, MA), and modified its shape from linear to curved L-shape for our experiment. Using external voltage supply, 6 kV was supplied to sharp needle for generating ionic wind toward collector Cu tube. After 24h of collecting duration, Cu collection tube was washed with methanol/water (1:1, vol./vol.) for subsequent nESI-MS. For nESI-MS, nESI tip was pulled from borosilicate glass capillary (0.86 mm I.D., 10 cm L) using micropipette Puller, P-97 (Sutter Instrument Co., Novato, CA, USA) and Ag wire electrode was inserted into pulled nESI tip. Parameters used on nESI-MS were as follows: 200  $^{\circ}$ C capillary temperature, 3 microscans, 60% S-lens voltage, and 1.5 kV (DC voltage). All the experiments were performed in positive mode and data were acquired and processed using Thermo Fisher Scientific Xcalibur 2.2 SP1 software. Tandem MS was processed with collision-induced dissociation (CID) in the range of 25-30 for analyte identification.



**Figure S1.** Photograph of apparatus for offline collection of ion-molecule reaction products.

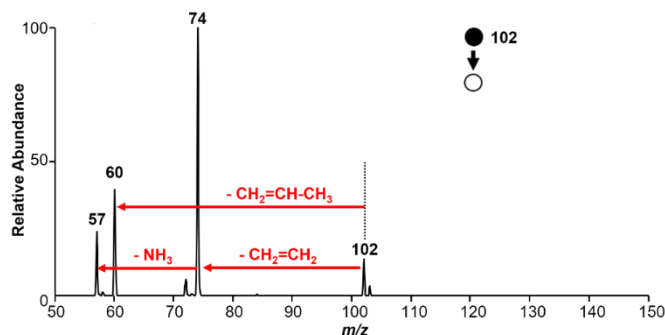
Liquid reactant (i.e., amine compounds) is placed in the reactant vials, which are inserted into a larger polyethylene (PE) container. The APCI needle is inserted at the top of the PE container. The hole in the APCI needle becomes the only exit through which analyte vapors are supplied from the reactant vials into the ionic wind. The copper tube is located approximately 10 mm distance away from the tip of the APCI needle and it is used to collect the gas-phase N-alkylation product once the copper tube is filled with water.

## 2. Comparison of survival yield (%) for two different configurations of plasma sources



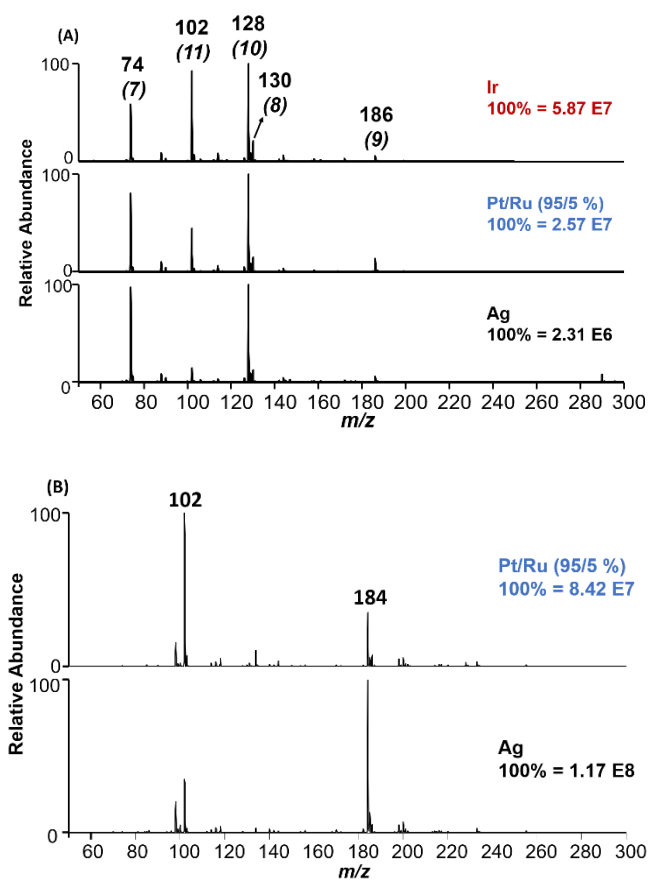
**Figure S2.** (A) contained-APCI where benzylamine vapor was added from the back of the plasma electrode and (B) traditional plasma-based ionization where the sample to be analyzed was placed in front of the plasma electrode. Survival yield (%) was calculated by comparing relatively intensity of  $m/z$  108 to the total intensity of ions  $m/z$  91, 106 and 108. Higher SY indicate softer ionization.

## 3. Tandem MS analysis of degradation product from n-butylamine N-alkylation reactions



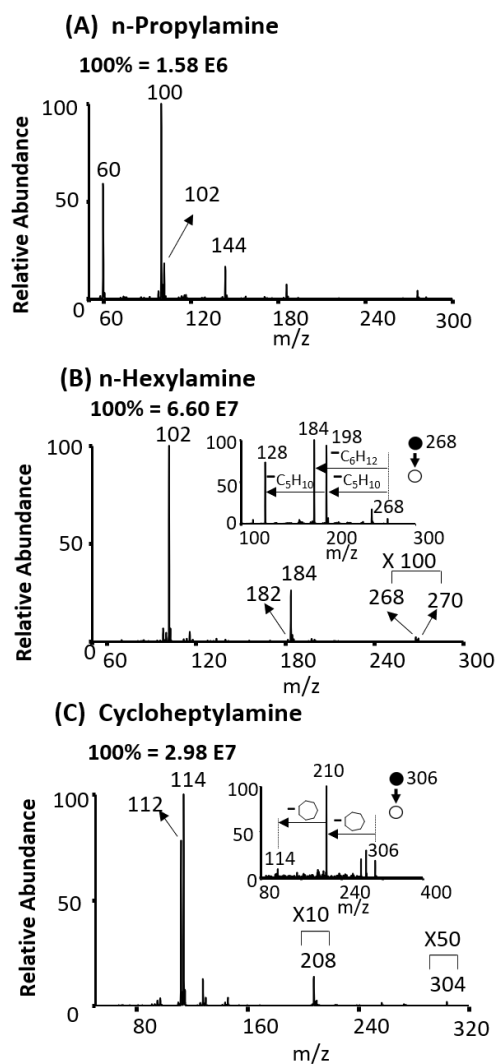
**Figure S3.** MS/MS of characterization of N-ethylbutan-1-amine (II,  $m/z$  102), which was produced from the decomposition of N-alkylated products (8,  $m/z$  130) from n-butylamine (7,  $m/z$  74).

#### 4. Surface effect studies utilizing Ag, Ir, and Pt/Ru electrodes



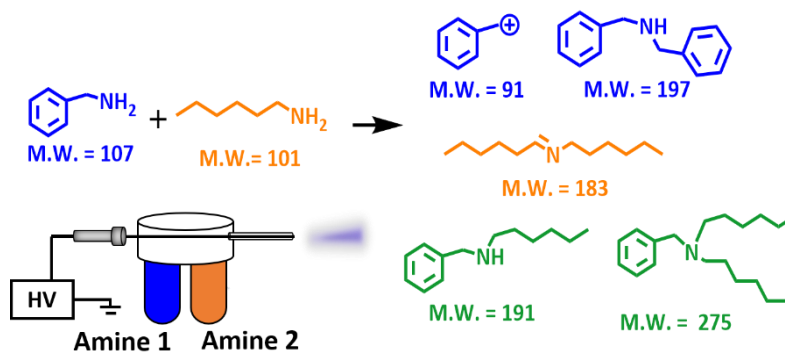
**Figure S4.** Surface effect studies show that Ag is an efficient discharge electrode for online reaction screening when compared to Ir and Pt/Ru (95/5 %). **(A)** Analysis of n-butylamine using Ir, Pt/Ru (95/5 %), and Ag. The peak at  $m/z$  102 is a decomposition product, which is most abundant on the reactive Ir electrode due to its high oxophilicity<sup>1</sup>. **(B)** The superiority of Ag to produce more gas-phase N-alkylated product is reaffirmed using n-hexylamine where higher relative abundance of ion at  $m/z$  184 is produced on Ag compared when using Pt/Ru electrode.

## 5. Online screening for other linear and cyclic aliphatic amines

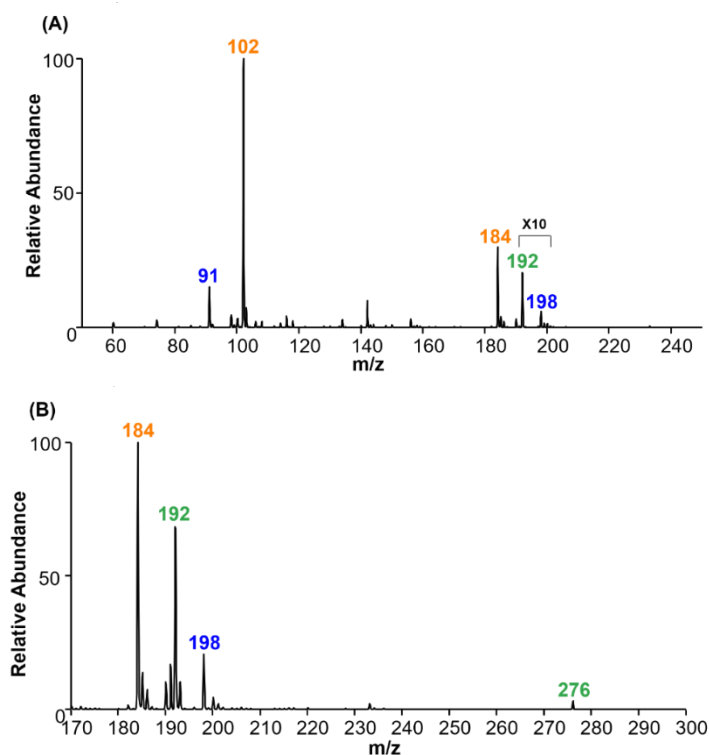


**Figure S5.** MS and MS/MS analysis of other linear and cyclic aliphatic amines tested on online contained-APCI screening experiments as followed: **(A)** n-propylamine, **(B)** n-hexylamine, and **(C)** cycloheptylamine.

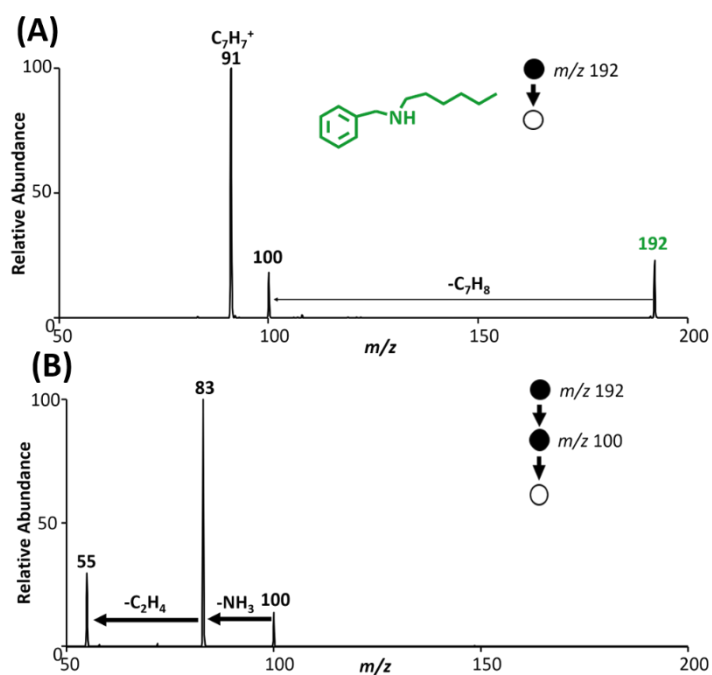
## 6. Cross-coupled N-alkylation between benzylamine and hexylamine



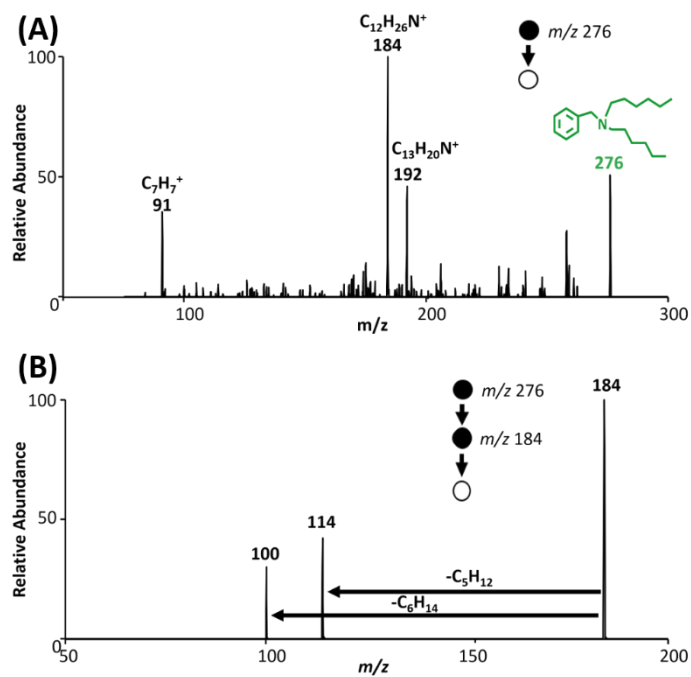
**Scheme S1.** Schematic illustration of cross-coupled N-alkylation products between two different amines (1: benzylamine and 2: hexylamine). Reactants were loaded in different reagent vials and headspace vapors reacted in real-time when a DC voltage was applied to the Ag electrode.



**Figure S6.** (A) Representative MS spectrum of cross-coupled N-alkylation of two different amines (benzylamine and hexylamine) using the online contained-APCI apparatus. Both self and cross-coupled N-alkylation were observed from experiment. (B) Zoom-in mass spectrum from (A) in the range of  $m/z$  = 170-300. Blue colored peaks represent products from benzylamine ( $m/z$  = 91, 108, and 198), orange colored peaks represent those from hexylamine ( $m/z$  102 and 184), and green colored show cross-coupled N-alkylation between benzyl- and hexylamine ( $m/z$  = 192 and 276). Tandem MS characterization of the cross-coupled products,  $m/z$  192 and  $m/z$  276 are provided in Figure S7 and Figure S8, respectively. Chemical structures corresponding to peaks are shown in Scheme S1.



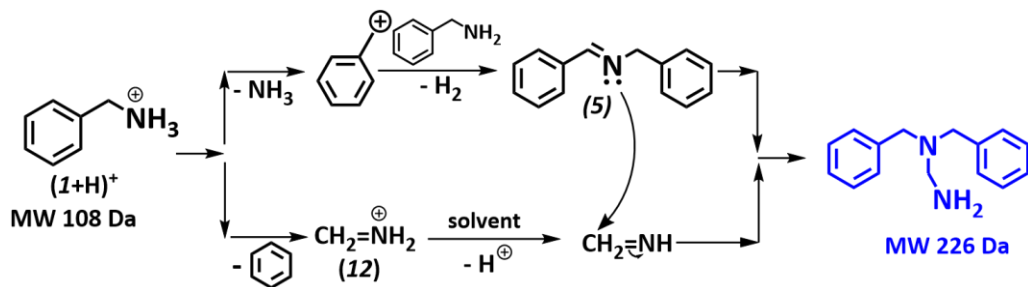
**Figure S7.** Annotated (A) MS<sup>2</sup> and (B) MS<sup>3</sup> of first cross-coupled N-alkylation species ( $m/z$  192) derived from benzylamine and hexylamine vapors in **Figure S6**.



**Figure S8.** Annotated (A) MS<sup>2</sup> and (B) MS<sup>3</sup> of second cross-coupled N-alkylation species ( $m/z$  276) derived from benzylamine and hexylamine vapors in **Figure S6**.

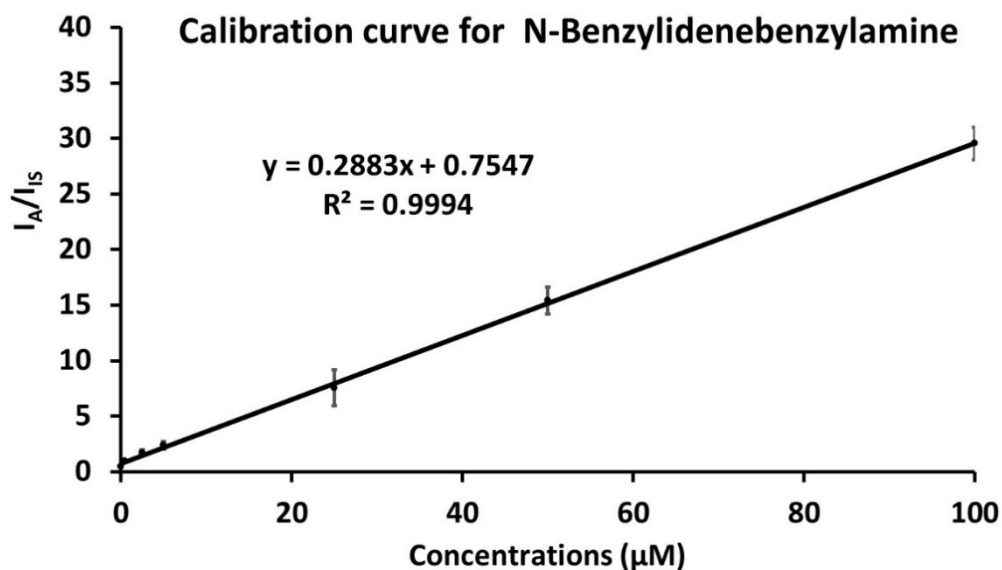


7. Possible mechanism of solution-phase reactions involving collected ionic species from the ionic wind



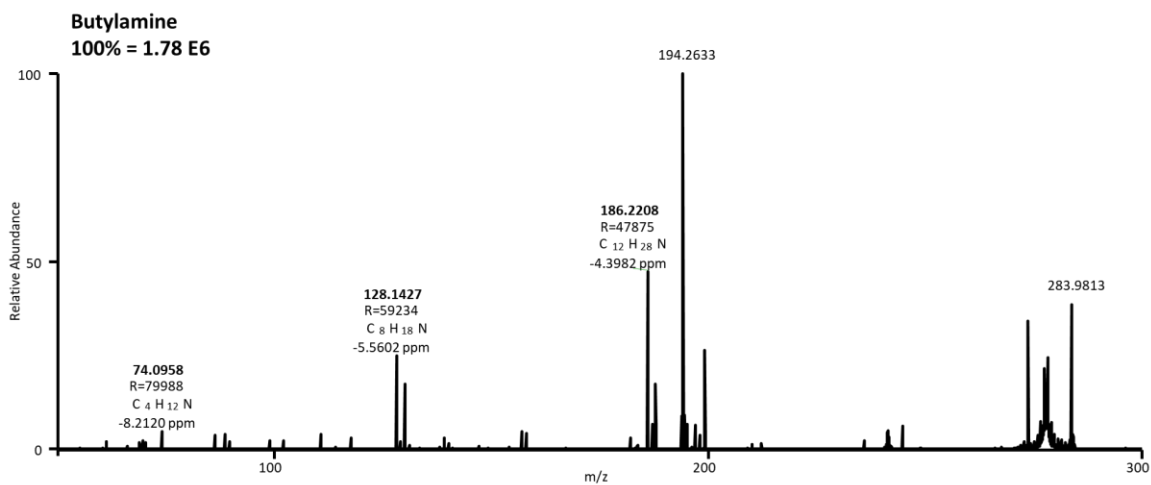
**Scheme S2.** Alternative solution-phase reaction pathway involving the collected ionic species from benzylamine in offline collection experiment. This pathway is not observed in our experiment as its  $m/z$  is not shown.

8. Estimation of the amounts of N-benzylidenebenzylamine collected from the gas-phase reaction using benzylamine vapor

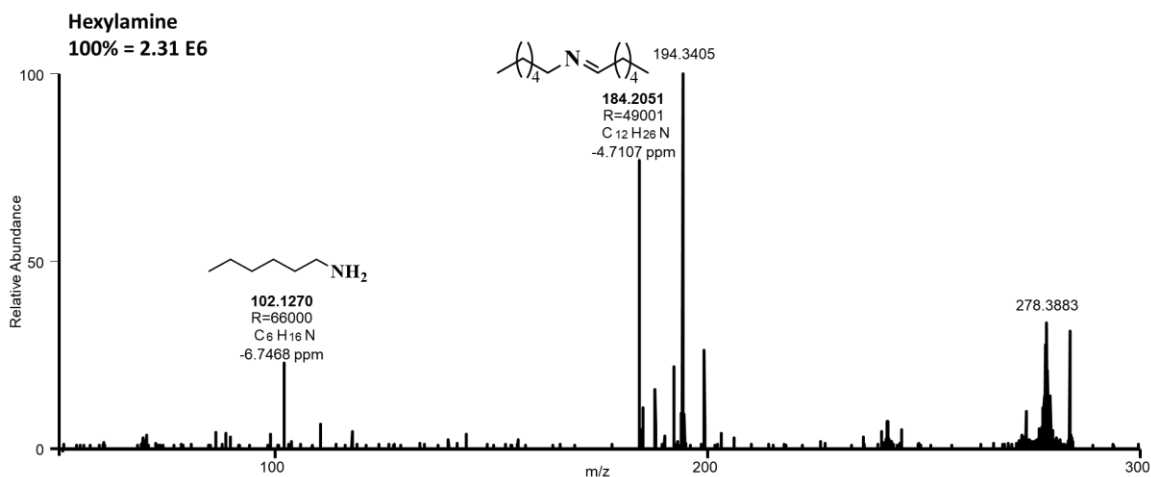


**Figure S9.** Internal calibration curve used in estimating the amounts of N-benzylidenebenzylamine (**5**,  $m/z$  196) collected in water during the offline experiment involving N-alkylation of benzylamine. Standard solutions of N-benzylidenebenzylamine was prepared for following concentrations: 0, 0.5, 2.5, 5, 25, 50, and 100  $\mu\text{M}$  and 1  $\mu\text{M}$  N-benzylideneaniline was used as an internal standard. The regression line equation generated was used to extrapolate amounts of N-benzylidenebenzylamine collected from the gas-phase reaction, yielding 74.3 mM, which was equivalent amount to 145.1  $\mu\text{g}$ . The volume (10  $\mu\text{L}$  aliquot solution) used for nESI-MS was corrected. Yield was estimated to be 6 % given that > 50 % of N-benzylidenebenzylamine (**5**) converted into N-benzyl-1-(methyleamino)-1-phenylmethanamine (**13**) during the residence in the water collecting solvent.

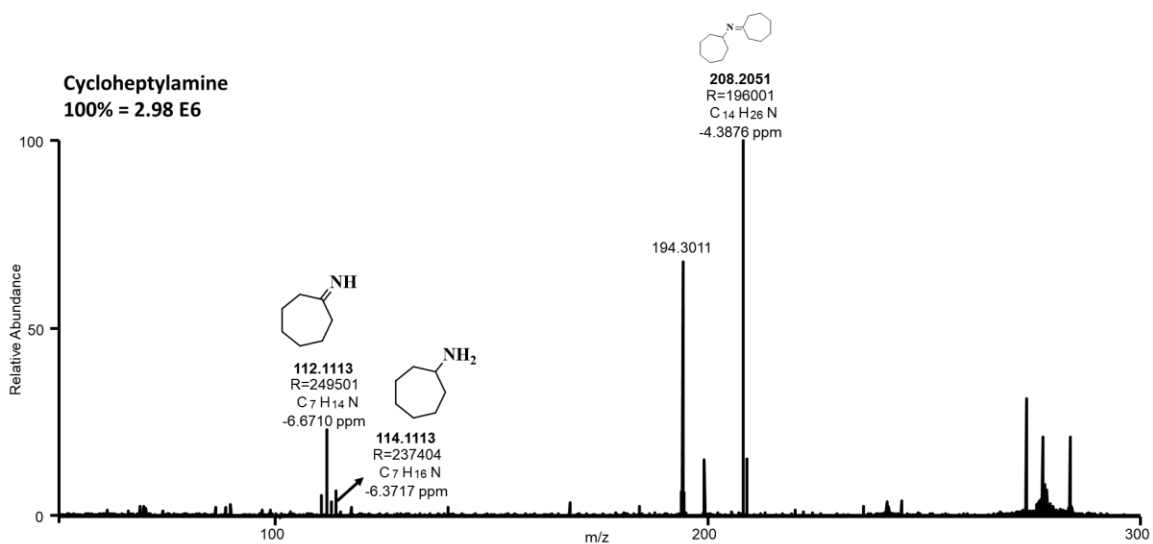
## 9. Orbitrap MS spectra of online screening N-alkylation of amines



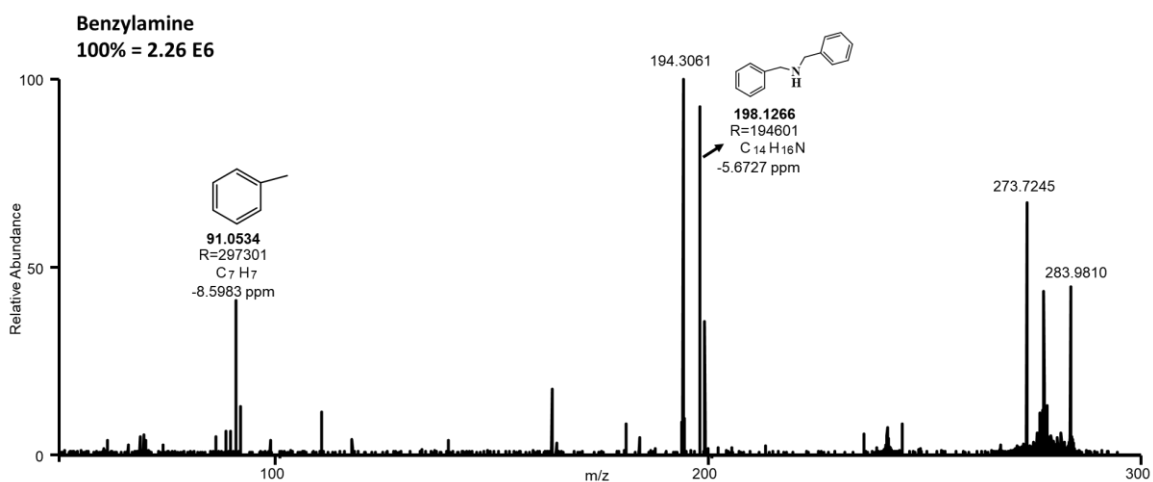
**Figure S10.** Exact mass analysis of N-alkylation products from n-butylamine using Orbitrap MS.  $m/z=194$ , 273, 278, and 283 exist as background peaks.



**Figure S11.** Exact mass analysis of N-alkylation products from n-hexylamine using Orbitrap MS.




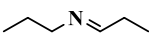

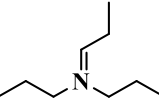
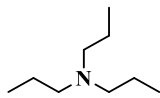
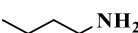


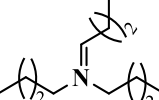
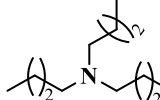
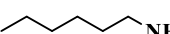


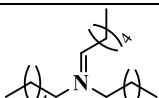
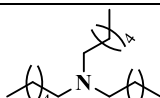
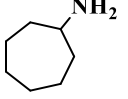
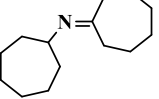
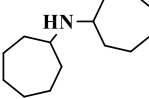
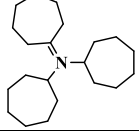
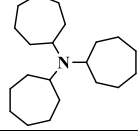
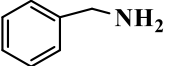
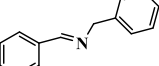
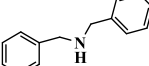
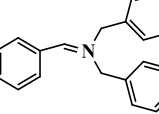
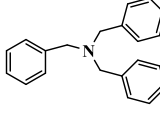
**Figure S12.** Exact mass analysis of N-alkylation products from cycloheptylamine using Orbitrap MS.



**Figure S13.** Exact mass analysis of N-alkylation products from benzylamine using Orbitrap MS.

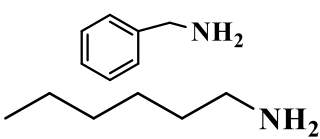
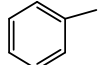
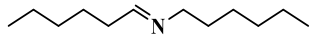
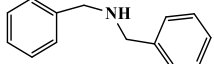
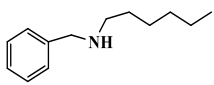
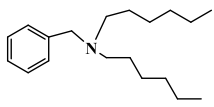
10. Chemical structures and relative abundances of products from online N-alkylation of all amines examined

**Table S1.** List of products from N-alkylation and their relative abundances from MS spectra.

Reactant	First N-alkyl. Imine		First N-alkyl. Amine		Second N-alkyl. Imine		Second N-alkyl. Amine	
	Product	<i>m/z</i> (Rel. %)	Product	<i>m/z</i> (Rel. %)	Product	<i>m/z</i> (Rel. %)	Product	<i>m/z</i> (Rel. %)
		100 (44.77)		102 (23.41)		142 (0.53)		144 (31.29)
		128 (84.39)		130 (11.98)		184 (0.19)		186 (3.44)
		184 (95.38)		186 (4.46)		268 (0.12)		270 (0.04)
		208 (72.66)		210 (23.97)		304 (2.17)		306 (1.20)
		196 (83.29)		198 (16.58)		286 (0.09)		288 (0.05)

**11. Chemical structures and relative abundances of products from online cross-coupled N-alkylation between benzylamine and hexylamine**

**Table S2.** Lists of products from N-alkylation between benzylamine and hexylamine and their relative intensities from MS spectra

Reactant	N-alkylation products	<i>m/z</i> (Rel.%)
		91(50.85)
		184(44.02)
		198(2.66)
		192(2.37)
		276(0.10)

**12. Reference**

(1) Danilovic, N.; Subbaraman, R.; Chang, K.-C.; Chang, S. H.; Kang, Y. J.; Snyder, J.; Paulikas, A. P.; Strmcnik, D.; Kim, Y.-T.; Myers, D.; Stamenkovic, V. R.; Markovic, N. M. Activity–Stability Trends for the Oxygen Evolution Reaction on Monometallic Oxides in Acidic Environments. *J. Phys. Chem. Lett.* **2014**, 5, 2474–2478.